Empirical analysis of partial discharge data and innovative visualization tools for defect identification under DC stress

Abdul Madhar, Saliha ; Mraz, Petr; Rodrigo Mor, Armando; Ross, Rob

DOI
10.1016/j.ijepes.2020.106270

Publication date
2020

Document Version
Final published version

Published in
International Journal of Electrical Power & Energy Systems

Electrical Power and Energy Systems 123 (2020) 106270

Contents lists available at ScienceDirect

Electrical Power and Energy Systems

journal homepage: www.elsevier.com/locate/ijepes

Empirical analysis of partial discharge data and innovative visualization tools for defect identification under DC stress

Saliha Abdul Madhar[a,b,*], Petr Mraz[b], Armando Rodrigo Mor[a], Rob Ross[a]

[a] Delft University of Technology, Mekelweg 4, 2628 CD Delft, the Netherlands
[b] HAEFELY AG, Birsstrasse 300, 4052 Basel, Switzerland

ARTICLE INFO

Keywords:
Partial discharge (PD)
Defect identification
Patterns
Pulse Sequence Analysis (PSA)

ABSTRACT

This paper presents several approaches to the analysis of partial discharge (PD) data. Three common defects namely corona, surface and floating electrode are studied with the goal of defect identification under DC stress conditions. One of the major concerns with DC-PD testing, is its non-repetitive/erratic pulse pattern. This paper, however, only deals with the repetitive stages of discharge that will allow the study of their resultant patterns and trends. Several unique features such as the formative trend in the probability plot of time between discharges for the three common defect types shows promise in the quest for defect identification under DC. Further, the paper also describes in which way a three-pulse PSA diagram cannot serve as a standalone figure and hence requires a change in perspective by either adding or reducing a dimension. The last part of the paper presents a test methodology to identify the discharge source based on various discharge features.

1. Introduction

PARTIAL discharge (PD) testing has become an indispensable tool in type testing and quality certification for AC applications in the past decades. It has come to be a part of several international standards such as the IEC, IEEE and other European standards. With the global boom of HVDC transmission, a similar application of PD under DC stress is a popular prospect. Though the relationship between PD under DC and ageing or quality is not very well-known yet, the ability to verify a system's fitness or quality through PD testing is treated with great anticipation. It is a known fact that the discharge activity under DC is more complex than AC. The charge transport mechanism under DC is influenced by several properties of the surrounding material media. Some influencing factors are conductivity, temperature, humidity, material bonding/structure, surface roughness, electron-traps and its associated energy. For the design of DC high voltage (HV) components, material properties, their DC response and a complete knowledge of the transition stages (during turn-on, turn-off and polarity reversal) are a pre-requisite [1]. Some stray discharge pulses may perhaps occur on DC-PD tests that are not concerned with PD activity associated with any defect but only from space-charge or other external factors. Hence these are often ignored. The standard IEC 65700-19-03:2014 for DC bushings only sets a limit on the number of pulses in the last 30 min of the 2-hour test [2]. The interim Cigré report of WG D1.63 explicitly states that the state-of-the-art, up to now can detect and barely differentiate between stray pulses and real PD but cannot yet perform defect identification or risk assessment through partial discharge tests under DC [3].

So far, the most popular means of studying and characterizing insulation defects under DC has been through Pulse Sequence Analysis (PSA) of the partial discharge pulses. It was first introduced by Hoof and Patsch in 1995 to study PD induced ageing under DC [4]. In later years, some other statistical parameters were studied with the object of creating unique defect fingerprints under DC [5,6]. Nevertheless, the fingerprints presented have failed to match the effectiveness of the Phase Resolved PD (PRPD) plots which revolutionized the AC asset diagnostic and maintenance business [7].

Research on DC partial discharges has either focused on the study and understanding of the discharge mechanism or purely on its statistical classification alone. The both lead to interesting results but do not provide a direct solution to defect identification. Therefore, this paper presents different approaches to partial discharge defect identification under DC stress conditions through various empirical analysis of the discharge data. The in-depth study of the individual defects presented here were conducted prior to the analysis in order to determine which discharge stage strongly represents the defect nature/character [8,9]. Characteristic features of every defect type were identified and are further used in this paper to generate visual patterns for defect recognition. The PD raw data (pulse stream) has been established to have

* Corresponding author.
E-mail address: S.AbdulMadhar@tudelft.nl (S. Abdul Madhar).

https://doi.org/10.1016/j.ijepes.2020.106270
Received 24 March 2020; Received in revised form 18 May 2020; Accepted 4 June 2020

contained discharge pulses only from a single defect with the help of additional optical measurements as were described in [9]. The goal of the contribution is to suggest means of DC defect identification that are both perceptive and practical.

2. Artificial PD defects: data collection

The three most common insulation defects namely protrusion, floating electrode and surface defect are studied experimentally using artificially created models in different laboratory arrangements. In order to verify the plausibility of the setup, tests have been carried out at different locations, using different voltage sources, connection components and external conditions. Discharge time series (data) has been recorded at all instances and a selected sample of the results are utilized to demonstrate the empirical analysis of Section 3. This section describes the generalized measuring circuit employed in data acquisition and the individual defect arrangements and their relevant features.

2.1. Generalized measuring setup

The electrical measuring setup is built based on the recommendations of the International Standards IEC 60270 [10]. The schematic of the measurement circuit is shown in Fig. 1. The half-wave rectifier with a large smoothing capacitor of 20 nF is used to generate DC voltage. The ripple on the output DC voltage has been measured to be below 0.4% up to 30 kV_{dc}. The polarity of DC voltage is changed based on the position of the diode. A high voltage blocking inductor (L_b) is used in series with the rectifier in order to improve the measuring sensitivity of the PD circuit. A 1.2 nF coupling capacitor (C_k) serves as the low impedance path for the high frequency (HF) discharge pulses as well as the part of the R||C voltage divider for DC voltage measurement. A measuring impedance (Z_m) otherwise referred to as a quadrupole (AKV 9310) is used to measure the PD pulses. The partial discharge detector DDX 9121b is used as the front end for all the measurements. It records the charge (pC), pulse rate, discharge current and voltage every second, providing a preliminary log of the entire PD test scheme.

The 'signal' output channel on the front panel of the DDX 9121b provides the possibility of data streaming through the connection of an external acquisition device. In this case, an oscilloscope with a measuring bandwidth (BW) of 250 MHz is used to continuously record the discharge pulse stream at a sampling speed of 10 or 20 MS/s. The AKV 9310 (quadrupole) has a measuring bandwidth of ~8 MHz together with the electrical measurement loop created by the 1.2 nF coupling unit. The DDX 9121b has optional input analog filter stages (Low-Pass ~ 2 MHz) to pre-condition the incoming pulse stream and discriminate them from external HF noise. These BW limitations create a complex interaction thereby influencing the resultant output pulse recorded by the oscilloscope. The lowered bandwidth influences the shape of the discharge pulse by making the pulse longer in time or slower in frequency.

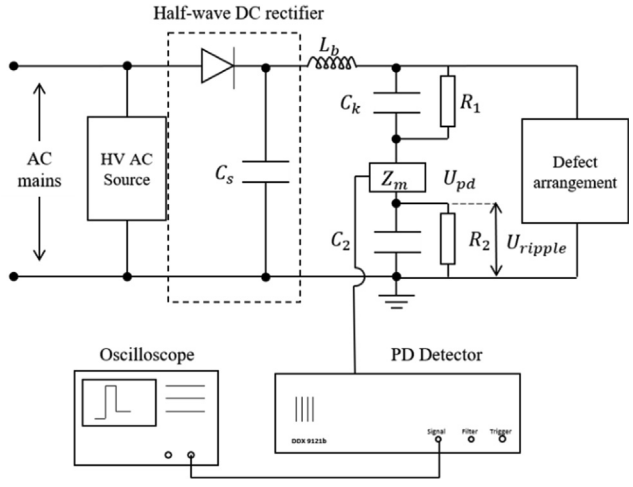

Fig. 1. Schematic of the electrical circuit for the DC partial discharge measurement.

However, since the PD pulses that occur within an industrial HV component are almost always limited in BW, and the analysis made in this contribution does not study the discharges based on pulse shape parameters, this feature has not been optimized. The second major influence of the low BW is on the maximum PD pulse rate that can be recorded reliably. Ideally, with the 2 MHz Low-Pass (LP) analog filter a pulse rate given by the Nyquist criteria ($f_{max} = f_S/2$) approaches 1 MHz. And in the case of DC partial discharges, with the exception of certain corona configurations (PD from protrusion), none of the other defects encounter this problem due to low repetition rates. The exceptional case of corona with exceeding pulse rates has been presented in detailed studies previously [9,11].

The circuit in its final form, excluding the defect arrangement is known to be PD-free in the test voltage range. Before the start of each test, the setup is calibrated in order to display the right value of charge (pC). A sample calibration pulse is recorded in advance to calibrate the pulse stream recorded using the oscilloscope. This is done in the post-processing phase using a set of specially developed algorithms on MATLAB platform.

2.2. PD defect models

2.2.1. Corona or protrusion in air

The corona defect is typically created as a point-plane arrangement as shown in Fig. 2(a). The distance between the needle and the plane is maintained at 25 mm with a needle tip diameter in the range of ∅50 − 100 μm. A detailed study of the corona stages in its different configurations were presented in [9]. Two cases of corona are presented in this paper, negative corona (or Trichel) and positive corona. The negative corona presented in Sections 3.1–3.3 belongs to the configuration with positive DC voltage and needle placed on ground plane. The pulse stream has been recorded at 8.7 kV_{dc}. While the positive corona presented in the same respective sections belongs to the configuration with positive DC voltage applied to the needle at HV. The pulse stream has been recorded at 6.5 kV_{dc}.

2.2.2. Surface discharge on dielectric-air interface

The surface discharge model is built as shown in Fig. 2(b). The dielectric sample is sandwiched between two electrodes with dimensions as mentioned in the figure. A spring is placed over the upper electrode plate to apply pressure over the sample to ensure good contact. The model is verified for surface PD based on its resultant PRPD pattern on AC voltage stress prior to DC-PD testing. The positive and negative surface discharge data measured with two different samples (Samples A and B) is presented in Sections 3.1–3.3. Sample A is polyethylene-based material and Sample B is resin impregnated pressboard. The pulse streams for sample A are recorded at +6.8 kV_{dc} and −6.5 kV_{dc} and that for sample B are recorded at +3.8 kV_{dc} and −4.7 kV_{dc}.

2.2.3. Floating electrode in air

The floating electrode arrangement has been constructed as shown in Fig. 2(c). The dimensions of the various relevant parts have been specified in the figure. A detailed study on the individual defect has been presented in [8] where is described the choice of the arrangement and the nature of the discharge stage. The model is verified for floating PD similar to the previous case by referring to its corresponding PRPD plot under AC. The floating electrode under positive and negative DC presented in Sections 3.1–3.3 are recorded at +29.5 kV_{dc} and −29.5 kV_{dc}.

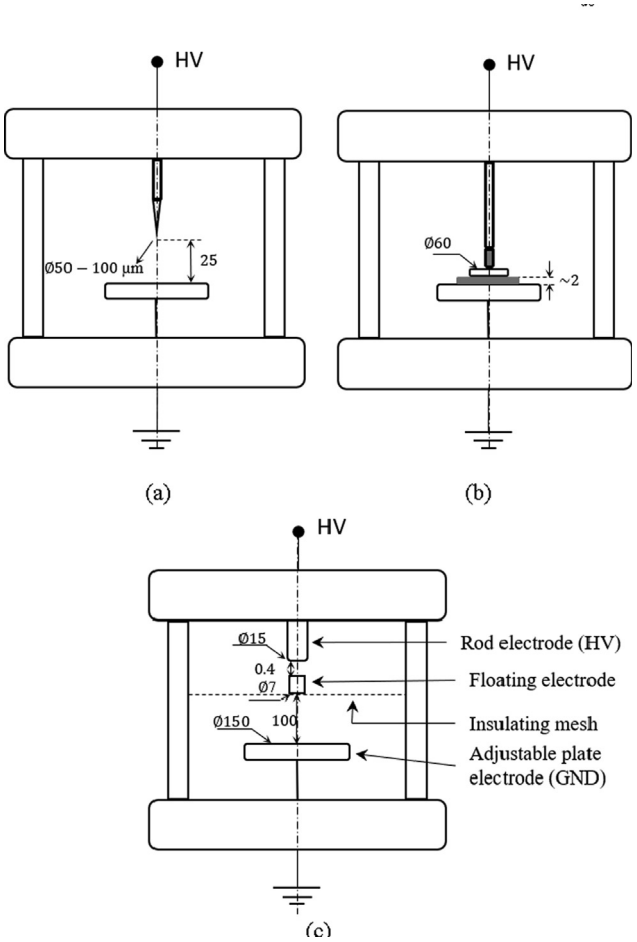

Fig. 2. Schematic of the artificial defect models (a) corona/ protrusion in air, (b) surface discharge on dielectric-air interface and (c) floating electrode defect in air. (all dimensions are in mm).

3. Data analysis

The discharge pulse stream recorded for the three PD defects is post-processed to acquire the values of discharge magnitude (with polarity) and time of discharge event. These two quantities serve as the basis of the analysis presented in the following sections. Details on the length of recorded data and the number of pulses (data points) are listed on Table 1.

3.1. Statistical analysis of discharge parameters

The statistical distribution of the discharge quantities is studied in this section. Two quantities namely, difference in magnitude of successive charge (ΔQ) and time between successive charge (Δt) as shown in Fig. 3 are considered. Both are normalized from 0 to 1 using the

Table 1
Details of the stream length and no. of pulses for each defect type.

Defect type	Test voltage [kV_{dc}]	Recording time [s]	No. of pulses
Pos. corona	+6.5	2.5	1239
Neg. corona	+8.7	0.23	30,000
Surface (sample A)	+6.8	120	1023
	−6.5	120	908
Surface (sample B)	+3.8	2.5	2484
	−4.7	10	2175
Floating electrode	+29.5	2.5	532
	−29.5	5	10,253

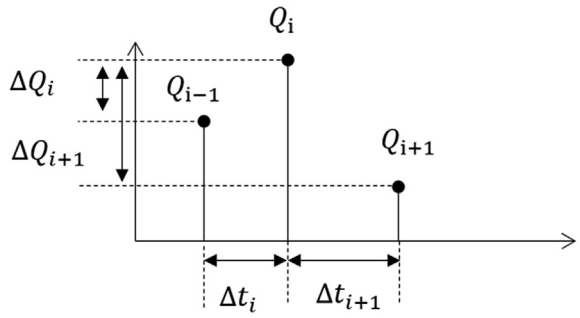

Fig. 3. An illustration of a typical PD pulse sequence acquisition showing the derived quantities of Δt and ΔQ, where subscript i represents the i^{th} pulse.

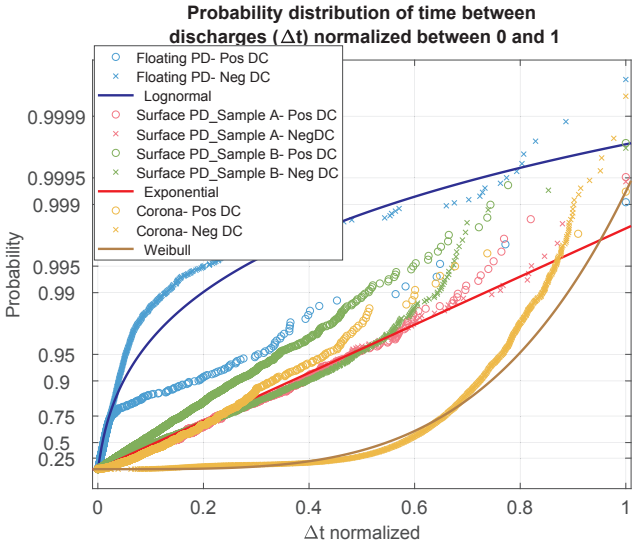

Fig. 4. Probability distribution of time between discharges (Δt) for various defects normalized between 0 and 1.

expression given in Eq. (1).

$$x' = \frac{\{x - min(x)\}}{\{max(x) - min(x)\}} \quad (1)$$

where x' is the normalized value and x is the actual value. An exponential distribution is used to construct the probability plots shown in Figs. 4 and 5. Fig. 4 shows the probability distribution of the normalized time between discharges (Δt) for various PD defect types. Three

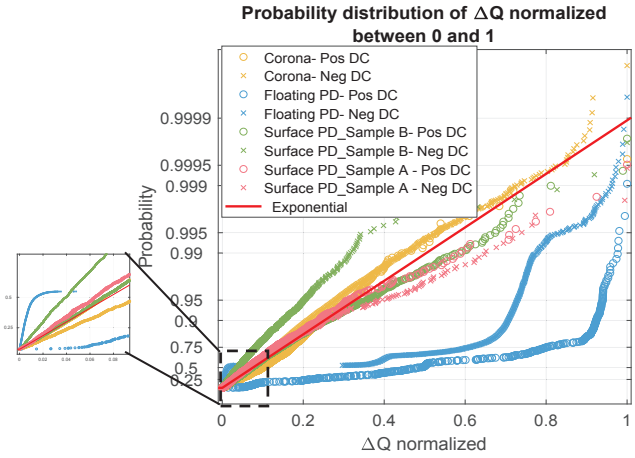

Fig. 5. Probability distribution of change in discharge magnitude (ΔQ) for various defects normalized between 0 and 1 (insert with zoom).

distinctive distributions can be seen on this figure. First, the probability distribution of floating electrode defect that follows a log-normal distribution. The defect under -DC discharges at a steady rate and the distribution of Δt values well represent/fit the lognormal curve. The floating defect under + DC on the other hand has a slow repetition rate and only up to 80% of the points fit the lognormal distribution while the tail on the upper end poorly fits the curve. Secondly, can be observed the exponential distribution of the surface discharge quantity of Δt. The surface defect tested for both samples A and B under both positive and negative DC showcases a similar distribution. The Δt distribution for positive corona also appears to follow an exponential distribution. Negative corona, however, follows a unique Weibull distribution. All the curves (lognormal, exponential and Weibull) are fitted for the showcased data series. Despite the poor fit of positive floating defect to the lognormal distribution and the likelihood of positive corona towards the exponential distribution rather than the Weibull distribution that negative corona follows, this analysis shows immense potential in aiding in the defect identification process.

The other discharge quantity that is available from a DC-PD measurement is the quantity of charge. A similar analysis is made on the ΔQ distributions of various defect sources with the same available data. The probability distribution of the normalized values of difference in magnitude of successive charge (ΔQ) are presented in Fig. 5.

Only two distinctive groups are seen on this plot. An exponential distribution of the normalized ΔQ values for corona and surface discharge, and a discontinuous distribution of the values of floating discharge. From [8] it can be noted that the floating PD under DC alternates between breakdown of the gap and corona over the floating body (in the repetitive discharge stage). And there is a disparity in discharge magnitudes of these two phenomena. This disparity reflects as the discontinuity in values of ΔQ. The initial part of the distribution follows a lognormal distribution (can be seen from the insert on Fig. 5) while the latter part follows a Weibull or double exponential curve.

3.2. Three dimensions to pulse sequence analysis

The plots of ΔQ_{i+1} vs. ΔQ_i and Δt_{i+1} vs. Δt_i (3-pulse PSA) commonly referred to as PSA plots often appear to have the same outlines/shapes for several defect types. For instance, the PSA plot for negative corona and surface discharge on positive DC shown in Fig. 6 appear nearly identical. However, both the discharge scenarios are dissimilar from each other and follow a unique discharge process. The advantages and

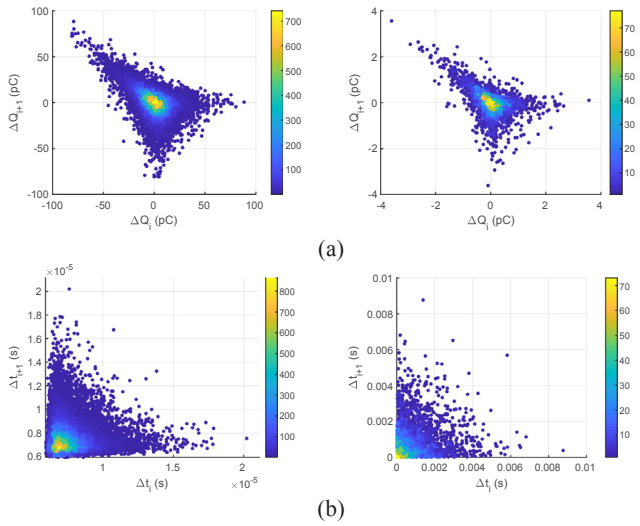

Fig. 6. The PSA plots of (a) ΔQ_{i+1}*vs.* $\Delta Q_i$for (left) negative corona and (right) positive surface discharge and (b) Δt_{i+1}*vs.* $\Delta t_i$for (left) negative corona and (right) positive surface defect. The heatmap shows the density of pulses.

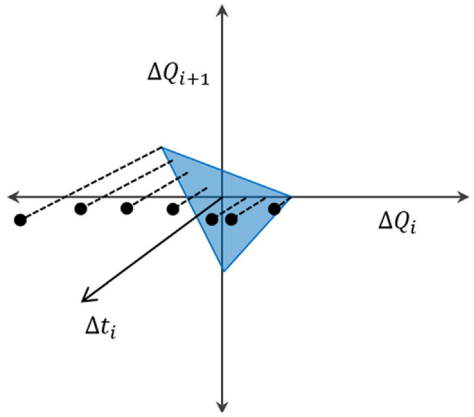

Fig. 7. Illustration of the three-dimensional PSA.

possible alternative solutions to this are evaluated in this section.

The PSA plot of ΔQ_{i+1} vs. ΔQ_i, plots the variation in discharge magnitude with no information about the pulse rate or time between the respective pulses. Similarly, the PSA plot of Δt_{i+1} vs. Δt_i plots the variation in time between discharges but with no information on the discharge magnitude of these respective pulses. On the contrary, a 2-pulse PSA, plot of Δt vs. ΔQ, includes both the quantities of change in discharge magnitude and pulse rate. However, is limited to the pulse sequence information of just two successive pulses. Therefore, if the goal is to represent the pulse sequence information of three successive pulses, the PSA plots of change in discharge magnitude and time need to be considered together to create a complete three dimensional (3-D) image as illustrated in Fig. 7. This would show each of the plots with a unique distribution without omitting the information of either quantities. For instance, the plots of negative corona and positive surface discharge shown in Fig. 6 are combined to form the three-dimensional PSA in Fig. 8.

It can be seen that the pulse distributions in 3-D are distinct from one and other. In order to highlight the difference, the curve-fitting tool in MATLAB is used to plot a plane for the given pulse distribution using a second order polynomial equation. The plane is not used to fit the data accurately but to demonstrate the differences in the density of the data on the two plots. The coefficients of the polynomial used in this process are presented in Table.2.

The phenomenon of partial discharge like any other in nature exhibits similarities/regularities but not absolute congruence. The goal of analysis should be to highlight or magnify the underlying regular pattern while minimizing the effect of outliners. However, the 3-pulse PSA tries to look into great detail towards the sequence in which the amplitudes of the pulses have emerged or the manner of evolution of the pulse rate. This magnifies the differences in the pulse stream creating a chaotic pattern in many cases. For instance, the corona discharge is the most stable in terms magnitude of charge and repetition rate. Instead of seeing a narrow scatter over a mean value, the 3-pulse PSAs in Fig. 6 displays an elaborate distribution. Seeming to reveal that the difference in pulse magnitudes change over a range of 0 to ± 100 pC (taken from the vertex of Fig. 6a). The magnitude variation of 100 pC might have taken place in a small percentage of the total pulses while the majority of the pulses were close to each other in magnitude. This needs careful examination by looking at the heat map of the plot and interpreting the density of pulses in each range. The three-dimensional PSA on one hand is complete and distinctive for various PD defects while on the other hand is complex to interpret and lacks intuitiveness. The 3-D plot suffers an added disadvantage as the three-dimensional plot also requires higher graphical processing power for its rendering and display. Therefore, due to the high level of complexity an alternative plot with weighted charge/time variables on the plot axis is proposed in the next section. The goal is to reach a level of effectiveness and simplicity

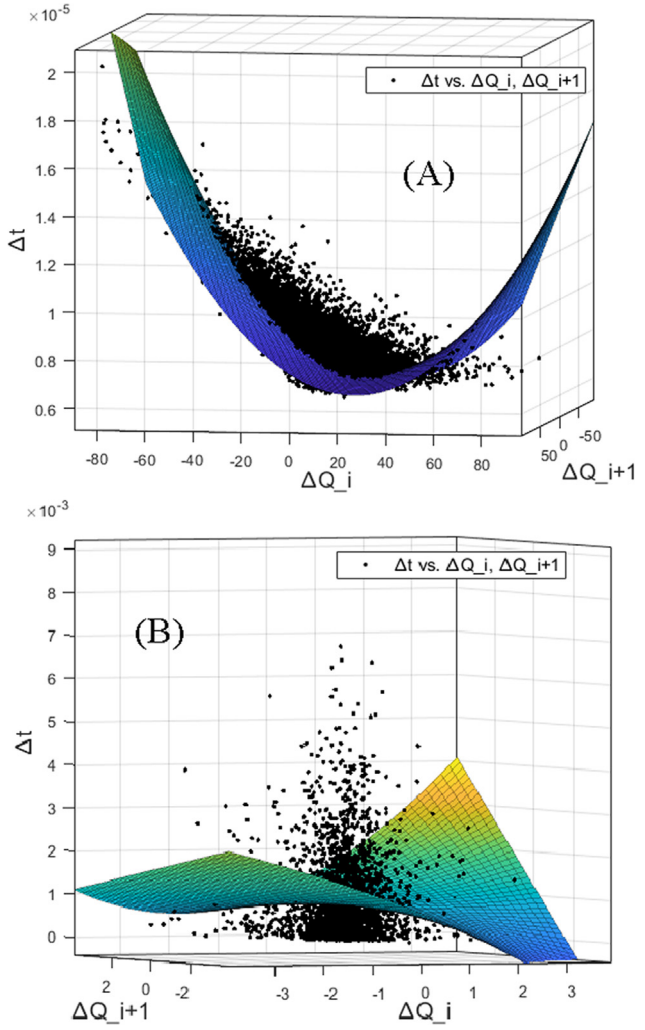

Fig. 8. The three-dimensional PSA plots of (a) negative corona and (b) positive surface defect.

Table 2
The coefficients of the polynomial used for curve fitting in Fig. 8.

f(x,y) = p00 + p10.x + p01.y + p20.x^2 + p11.xy	
Negative corona	p00 = 7.314e-06
	p10 = −4.59e-08
	p01 = 2.43e-08
	p20 = 1.16e-09
	p11 = −5.91e-10
Positive surface	p00 = 8.19e-04
	p10 = −3.92e-05
	p01 = 2.11e-05
	p20 = 4.18e-05
	p11 = 7.79e-05

comparable with the PRPD diagrams in AC where the outline/shape of the pattern is sufficient to distinguish various dielectric defects. Instead of requiring expert examination of multiple aspects prior to identification of defect type.

3.3. Weighted pulse sequence analysis (WePSA)

As described in the previous section, the 3-pulse PSA plots cannot be used as standalone plots since they either lack information on time or magnitude of charge. In order to have information on both change in time and change in charge magnitude on the same plot, one of the plot

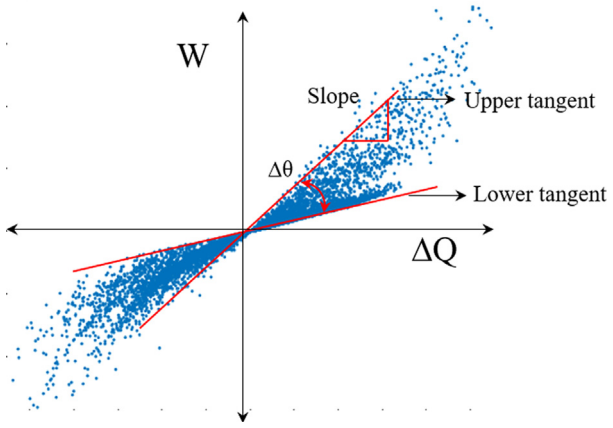

Fig. 9. An example to illustrate the features of a weighted PSA plot of weighted quantity W vs. change in discharge magnitude (ΔQ).

axis is used to represent a weighted quantity (represented by the variable W). The plot also helps minimize the effect of minor differences in the magnitude of discharge and discharge rate. And two plots are created, weighted with respect to time between discharges (W vs. Δt) and weighted with respect to change in discharge magnitude (W vs. ΔQ). The weighted quantity W is the product of the two quantities (ΔQ and Δt). It is derived as shown in Eq. (2).

$$W_{i=1toN} = \Delta Q_i \times \Delta t_i \tag{2}$$

where N is the number of discharge pulses in the given recorded stream. As the weighted quantity is a product of two other pulse parameters, the plot helps minimize the effect minor differences in the magnitude and rate of the discharge. Only the extreme/large differences in magnitude and rate outline the pattern. The following sections describe the features of the plots in more detail.

3.3.1. Plot of W vs. Δq

To illustrate the meaningfulness of the plot a sample weighted PSA plot of W vs. ΔQ is shown in Fig. 9. The slope and dispersion over the red lines shown on the figure can be derived as follows.

$$Slope = \tan\theta = \frac{dW}{d\Delta Q} = \frac{d(\Delta Q.\ \Delta t)}{d\Delta Q} = \Delta t \tag{3}$$

$$dispersion = slope_1 - slope_2 = \Delta t_1 - \Delta t_2 = d(\Delta t) \tag{4}$$

The plot for negative corona shown in Fig. 11(a) shows a very narrow scatter in the values of Δt which is representative of the corona Trichel pulse cluster that have almost a constant rate. On the contrary, the surface discharge pattern in Fig. 11(i) and Fig. 11(k) exhibit a full range variation from zero upwards to a maximum value which is depictive of the randomness in the surface discharge process. A unique form of asymmetry is seen the pattern of floating discharge shown in Fig. 11(e) and (g). This arises from the nature of the discharge which switches between breakdown of the gap and corona over the floating electrode (in the repetitive stage). The floating electrode defect exhibits a peculiar characteristic wherein a large breakdown pulse is followed by a series of small corona pulses and this pattern repeats itself. This imbalance in density of large vs. small pulses leads to an asymmetry in its discharge pattern. The similarity in the pattern of positive corona and surface discharge is dealt with at the end of the chapter.

In conclusion, the following set of inferences can be drawn from the weighted PSA plots of W vs. ΔQ:

Plot of W vs. ΔQ

I. The dispersion in the scatter plot of W vs. ΔQ is the dispersion in the value of Δt.
II. The slope of the external tangent enclosing the distribution gives

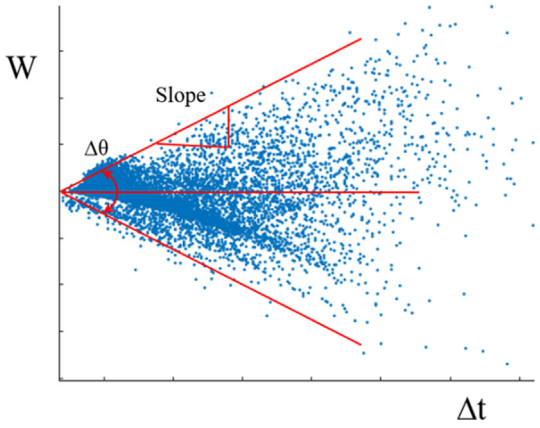

Fig. 10. An example to illustrate the features of a weighted PSA plot of weighted quantity W vs. time between discharges (Δt).

the smallest and largest values of Δt.

III. The symmetry in the diagram depicts that the variation in Δt is regular and does not follow a specific scheme. While on the contrary, an asymmetry such as in Fig. 11(e) and (g) shows multiple discharge process occurring systematically causing the data to group in a unique fashion.

3.3.2. Plot of W vs. Δt

The weighted PSA plot of W vs. Δt is shown in Fig. 10, the slope and dispersion over the red lines shown in the figure can be derived as follows.

$$Slope = \tan\theta = \frac{dW}{d\Delta t} = \frac{d(\Delta Q.\ \Delta t)}{d\Delta t} = \Delta Q \tag{5}$$

$$dispersion = slope_1 - slope_2 = \Delta Q_1 - \Delta Q_2 = d(\Delta Q) \tag{6}$$

That is the dispersion in the plot of W vs. Δt depicts the scatter in the values of ΔQ. In this case, the nature of the defect can be inferred from the axis of distribution. In case of corona there is a point distribution (shown in red in Fig. 11(b)) over W equal to zero, which would mean the quantity ΔQ variates about zero. Similarly, for surface PD (shown Fig. 11(j) and (l)) it is distributed symmetrically over the horizontal axis with a dispersion, $\Delta\theta$. Which indicates that the change in discharge magnitude in case of surface discharge is randomly distributed between zero and a maximum value defined based on the slope of the external tangent enclosing the distribution. The plots for floating discharge display an asymmetrical distribution due the systematic switching between the gap breakdown and corona over floating body.

In conclusion, the following set of inferences can be drawn from the weighted PSA plots of W vs. Δt:

Plot of W vs. Δt

I. The dispersion in the scatter of W vs. Δt gives the dispersion in the values of ΔQ.

II. The slope of the external tangent enclosing the distribution gives the largest values of ΔQ (positive/increasing trend or negative/decreasing trend).

III. Based on the axis of symmetry of the distribution, the nature of the discharge is determined (point symmetry, horizontal line symmetry, asymmetry with multiple clusters).

The weighted PSA plots for positive corona and surface discharge shown in Fig. 11 appear to be similar. The repetitive stage of positive corona (self-sustaining discharge state [9]) which is unlike Trichel seems to have similarities with the process of surface PD. However, the plot of repetition rate of the charge (N vs. Q) for the two defect sources are dissimilar. In case of positive corona, the range of discharge

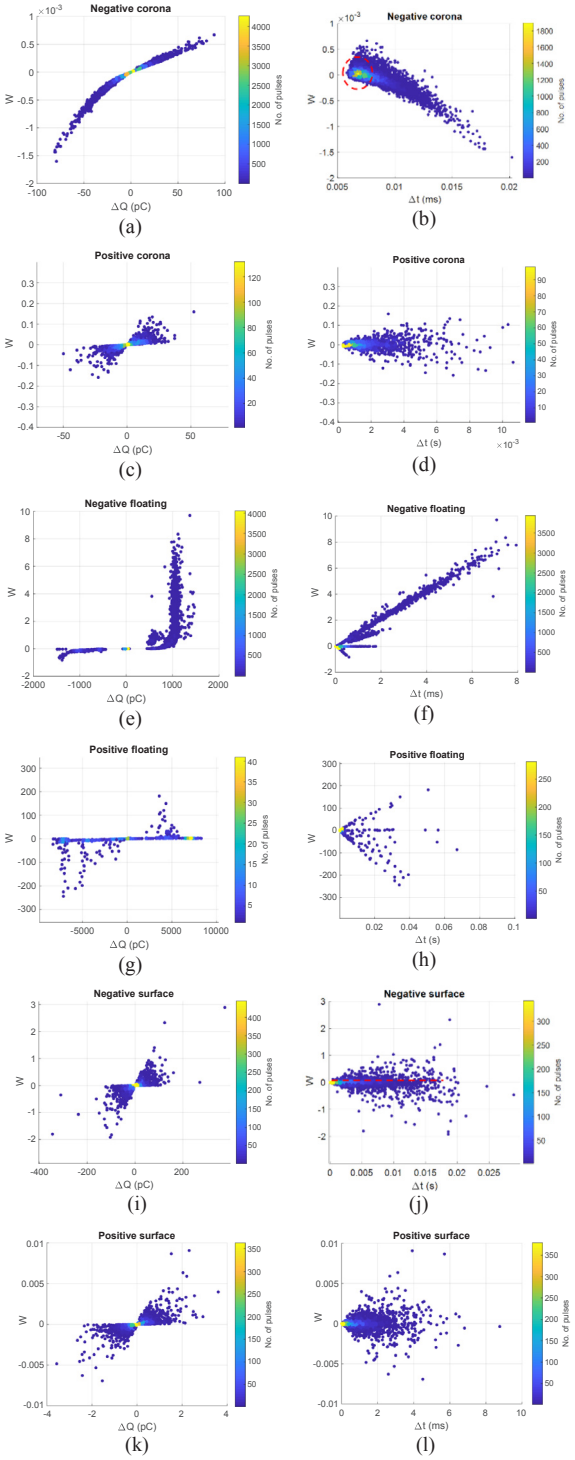

Fig. 11. The weighted pulse sequence plots (left column) W vs. ΔQ (right column) W vs. Δt, (a) & (b) Negative corona, (c) & (d) Positive corona, (e) & (f) Floating electrode on -DC, (g) & (h) Floating electrode on + DC, (i) & (j) Surface PD on -DC (Sample B), (k) & (l) Surface PD on + DC (Sample B).

magnitude varies over a median value as shown in Fig. 12(a). However, in the case of surface defect the magnitude of discharges varies from the smallest value possible to be measured (the charge threshold, Q_{th} set by the measuring system) to a maximum value.

In the first assessment of sorts, the weighted PSA plots appear to reveal more information than the, 2-pulse PSA, 3-pulse PSA, 3-D PSA and are more perceptive and stable. They possess visible differences and exhibit unique patterns for various defect types and hence may be a

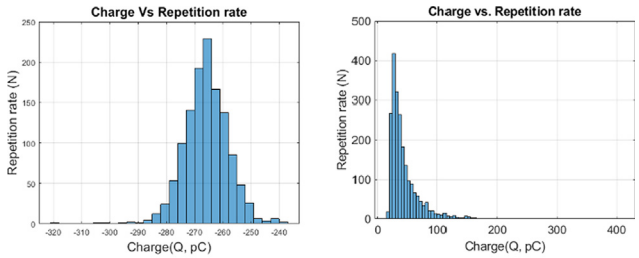

Fig. 12. Plot of charge (Q) vs. repetition rate (N) for (a) Corona on + DC and (b) Surface PD on -DC.

suitable alternative to the latter.

4. Discussion

Defect identification under DC stress has gained tremendous traction in the recent years due to a wide spectrum of new DC applications. The ability to qualify the insulation quality and fitness of DC systems is the goal of partial discharge testing. So far partial discharges under DC have been treated as insufficient to produce a repeatable and well-shaped pattern due to their low pulse rates and erratic nature. However, several defect cases, such as the ones discussed in this paper, discharge at a stable rate (comparable to AC). This raises the significance of defect identification under DC with the aid of visual tools. Defect identification not just provides insight into the type of insulation system defect but also broadens the fundamental understanding on the insulation's DC behavior. This paper investigates several ways of analyzing discharge data under DC, exploring the possibilities of the most promising visual tool that is closest to the AC-PRPD diagrams. Based on the presented visual tools a decision tree is devised to distinguish between the different defect types. The flow chart shown in Fig. 13 categorizes the repetitive PD pulses using the weighted PSA plots (WePSA). The key towards visual pattern identification, is the possibility of recording sufficient number of pulses that will produce a pattern with adequate contrast. Therefore, the first decision block on the flow chart looks for selection of 'measurable and repetitive PD pulses'. In some cases, the PD pulses may be smaller in amplitude so that they are below the noise threshold of the acquisition system. In these cases, it will not be probable to build visual patterns with such an acquisition stream. In other cases, The PD pulse stream is non-recurrent, i.e. such as the singular pulses in a floating electrode defect or the pulse-free zone of corona. In these cases, the non-repetitive nature of the pulses, renders the acquisition ineffective due to lack of sufficient pulses. For the defect conditions that can be suitably measured and are repetitive in nature, WePSA plots are used in their classification. A narrow scatter range of Δt in the plot of W vs. ΔQ along with a point distribution around $W = 0$ in the plot of W vs. Δt is indicative of negative corona. A double check can be made by verifying the probability distribution of Δt and the unique trend in the correlation between $Q_{i+1}$and Δt_{i+1} [9]. The random/wide Δt scatter in the plot of W vs. ΔQ and a line distribution about the $W = 0$ intercept in the plot of W vs. Δt is indicative of a surface defect or positive corona. One or the other can be confirmed based on the distribution of Q (plot of N vs. Q). Floating discharge under DC has several unique features [8].

These translate in to well-structured, multiple clusters on the weighted PSA. The plot of Δt_i vs. Δt_{i+1} and the probability distribution of the values of Δt can also help verify the presence of the defect [8]. However, outside the repetitive discharge stage, it is rather complex to identify and isolate the defect. The floating electrode would breakdown over its gap once and then remain charged at the given DC voltage, unless the voltage is increased sufficiently to cause the next breakdown. Therefore, singular pulses at every increasing voltage level may indicate towards the presence of a floating electrode defect. The discharge process is described in depth in [8]. Similarly, no discharge is measured in case the defect is in the pulse-free zone of corona. This is dealt with in detail in [9].

Currently, the flow chart is limited to the three common defect types studied in the paper (corona, surface and floating electrode). With a growing database of defect data, the flow chart can be developed to adapt to several features of specific discharge sources and provide a comprehensive analysis on the nature of the discharge.

5. Conclusions

The paper summarizes the PD patterns obtained from three different partial discharge defects. It selects the data for processing based on previous studies [8,9] that designate a specific discharge characteristic to the particular defect configuration. For instance, the repetitive stage of floating electrode and the self-sustaining positive corona that are unique features based on which the defect could be identified are utilized in this paper. The following points recapitulate the various sections of the paper.

- It presents the unique statistical distribution of the quantity 'Δt' for three different defects, except positive corona that closely resembles the surface discharge defect. This could serve as a diagnostic tool in PD defect identification.
- The new perspective to PSA, demonstrating the possibility of a three dimensional or 3D-PSA plot by combing two plots has been proposed.
- The novel weighted PSA (WePSA) plots proposed in the paper are not only visibly distinctive but also perceptive and simple to interpret to a great extent.
- The decision chart presented in the last section of the paper devises a diagnostic procedure by means of which one can investigate the nature of discharge under DC stress conditions.

It is understood that PD under DC does not manifest itself as clearly and systematically as under AC (repetitive with each voltage cycle). And even in conditions in which it does, a single figure/pattern may not be entirely sufficient to determine the source. Therefore, the multiple patterns and methods of analysis presented in this paper are proposed with the final goal of implementation in the PD diagnostic phase aiding in the identification of the PD defect type. The results presented show great promise, especially with the novel 'Weighted PSA' plots (WePSA patterns) that come a step closer to the DC version of PRPD.

CRediT authorship contribution statement

Saliha Abdul Madhar: Conceptualization, Methodology, Formal analysis, Investigation, Writing - original draft. **Petr Mraz:** Writing - review & editing, Supervision, Project administration, Validation, Resources. **Armando Rodrigo Mor:** Writing - review & editing, Supervision, Project administration, Validation. **Rob Ross:** Supervision.

Declaration of Competing Interest

The authors declare that they have no known competing financial interests or personal relationships that could have appeared to influence the work reported in this paper.

Acknowledgment

This work has partially received funding from the European Union's Horizon 2020 research and innovation programme under the Marie Sklodowska-Curie grant agreement No. 676042.

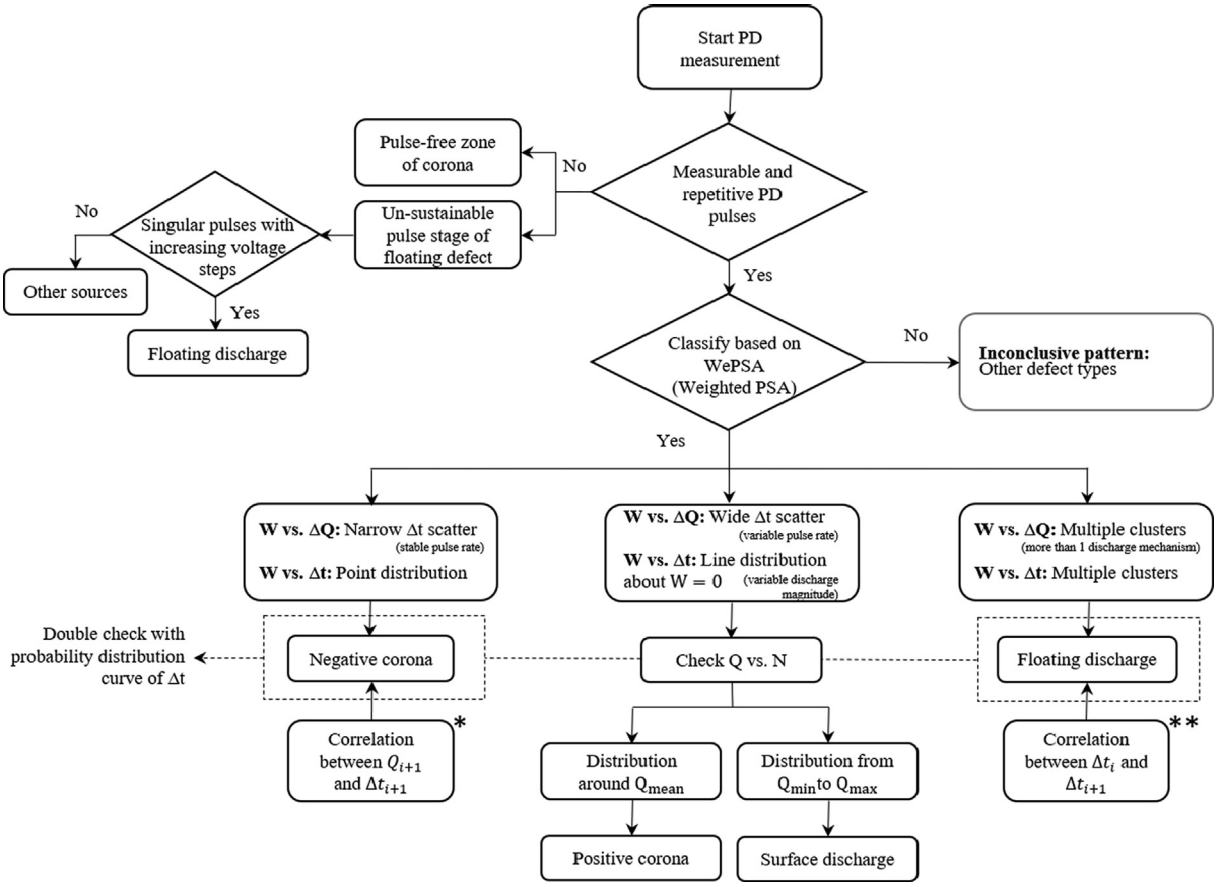

Fig. 13. Flow chart identifying the defect sources based on the weighted PSA plots. *The unique relationship between the quantities of charge (Q_{i+1}) and time to discharge (Δt_{i+1}) have been presented in [9] **The unique discharge patterns of Δt_i vs. Δt_{i+1} for floating electrode defect are presented in [8].

References

[1] Christen T. Characterization and robustness of HVDC insulation. In: 2013 IEEE international conference on solid dielectrics (ICSD), Bologna; 2013. p. 238–41.
[2] Standard IEC 65700-19-03:2014. "Bushings for DC application," International Standard, International Electrotechnical Commission (IEC); 2014.
[3] Abbasi A, et al. Progress on partial discharge detection under DC voltage stress. International colloquium on power transformers & reactors CIGRE, New Delhi; 2019.
[4] Hoof M, Patsch R. Pulse-sequence analysis: a new method for investigating the physics of PD-induced ageing. IEE Proc – Sci, Meas Technol 1995;142(1):95–101.
[5] Morshuis P, Hoogenraad G. Partial discharge diagnostics for DC equipment. In: Conference record of the 1996 IEEE international symposium on electrical insulation, Montreal, Quebec, Canada, vol. 1; 1996. p. 407–10.
[6] Morshuis PHF, Smit JJ. Partial discharges at DC voltage: their mechanism, detection and analysis. IEEE Trans Dielectr Electr Insul April 2005;12(2):328–40.
[7] Fruth B, Niemeyer L. The importance of statistical characteristics of partial discharge data. IEEE Trans Electr Insul Feb. 1992;27(1):60–9.
[8] Abdul Madhar Saliha, Mraz Petr, Rodrigo Mor Armando, Ross Robert. Physical interpretation of the floating electrode defect patterns under AC and DC stress conditions. Int J Electr Power Energy Syst 2020;118:105733. https://doi.org/10.1016/j.ijepes.2019.105733.
[9] Abdul Madhar S, et al. Study of corona configurations under DC conditions and recommendation for an identification test plan. Int J Electr Power Energy Syst, vol. 118: 105820; 2020.
[10] Standard IEC60270. "High-voltage test techniques–Partial discharge measurements, " International Electrotechnical Commission (IEC); 2000.
[11] Abdul Madhar S, Wenger P. Simultaneous electrical and UHF measurement of DC-PD from point-plane defect. Proceedings of the 21st international symposium on high voltage engineering (ISH), Springer, book chapter; 2019. p. 991–1003.

Saliha Abdul Madhar was born in Chennai, India. She received her MSc in Electrical Sustainable Energy with a special focus on High Voltage techniques, from the Delft University of Technology, the Netherlands, in 2017. She is currently working with HAEFELY AG in Basel, Switzerland while pursuing her PhD with the Delft University of Technology. Her PhD focusses on the study of Partial Discharge phenomenon under DC stress. Her research interests include HV Asset monitoring and diagnostics and dielectric phenomenon in HVDC.

Petr Mraz received his PhD degree in Diagnosis of Electrical Devices from the University of West Bohemia in Pilsen, Czech Republic in 2014. His research specifically focused on Partial Discharge Measurement and Evaluation. He currently works at HAEFELY AG, where he started in 2014 as an Application Engineer but has since become a Product Manager and Development Project Leader primarily responsible for Partial Discharge product line. He is a member of several CIGRE working groups and the IEC 60270 maintenance team.

Armando Rodrigo Mor is an Industrial Engineer from Universitat Politècnica de València, in Valencia, Spain, with a Ph.D. degree from this university in electrical engineering. In Spain, he joined and later led the High Voltage Laboratory and the Plasma Arc Laboratory of the Instituto de Tecnología Eléctrica in Valencia, Spain. Since 2013 he is an Assistant Professor in the Electrical Sustainable Energy Department at Delft University of Technology, in Delft, Netherlands. His research interests include monitoring and diagnostic, sensors for high voltage applications, high voltage engineering, space charge measurements and HVDC.

Robert Ross is professor at TU Delft, director of IWO (Institute for Science & Development, Ede), professor at HAN University of Applied Sciences and Asset Management Research Strategist at TenneT (TSO in the Netherlands and part of Germany). At KEMA he worked on reliability and post-failure forensic investigations. His interests concern reliability statistics, electro-technical materials, sustainable technology and superconductivity. For energy inventions he was granted a SenterNovem Annual award and nominated Best Researcher by the World Technology Network. He recently wrote the Wiley/IEEE book "Reliability Analysis for Asset Management of Electric Power Grids" based on experience with utilities and navy